

This article is a non-reviewed preprint published at EarthArXiv and was submitted to Frontiers in Earth Science (Cryospheric Sciences) for peer-review.

Exceptional retreat of Kangerdlugssuaq Glacier, east Greenland, between 2016 and 2018

Stephen Brough^{1*}, J. Rachel Carr¹, Neil Ross¹, and James M. Lea²

¹School of Geography, Politics, and Sociology, Newcastle University, Newcastle upon Tyne, NE1 7RU, UK

² Department of Geography and Planning, School of Environmental Sciences, University of Liverpool, Liverpool, L69 7ZT, UK

*** Correspondence:**

Stephen Brough
stephen.brough@ncl.ac.uk

Exceptional retreat of Kangerdlugssuaq Glacier, east Greenland, between 2016 and 2018

1 **Stephen Brough^{1*}, J. Rachel Carr¹, Neil Ross¹, and James M. Lea²**

2 ¹School of Geography, Politics, and Sociology, Newcastle University, Newcastle upon Tyne, NE1
3 7RU, UK

4 ² Department of Geography and Planning, School of Environmental Sciences, University of
5 Liverpool, Liverpool, L69 7ZT, UK

6 *** Correspondence:**

7 Stephen Brough

8 stephen.brough@ncl.ac.uk

9 **Keywords: Greenland Ice Sheet, marine-terminating glaciers, basal topography, ice discharge,**
10 **mass balance, glacier retreat, sea level rise, remote sensing.**

11 **Abstract**

12 Kangerdlugssuaq Glacier is one of Greenland's largest tidewater outlet glaciers, accounting for
13 approximately 5 % of all ice discharge from the Greenland Ice Sheet. In 2018 the Kangerlussuaq ice
14 front reached its most retreated position, since observations began in 1932. We determine the
15 relationship between retreat and: (i) ice velocity; and (ii) surface elevation change, to assess the
16 impact of the retreat on the glacier trunk. Between 2016 and 2018 the glacier retreated ~5 km and
17 brought the Kangerlussuaq ice front into a major (~15 km long) overdeepening. Coincident with this
18 retreat, the glacier thinned as a result of near-terminus acceleration in ice flow. The subglacial
19 topography means that 2016-18 terminus recession is likely to trigger a series of feedbacks between
20 retreat, thinning and glacier acceleration, leading to a rapid and high-magnitude increase in discharge
21 and sea level rise contribution. Dynamic thinning may continue until the glacier reaches the upward
22 sloping bed ~10 km inland of its current position. Given the complexity and scale of the processes
23 involved, such changes will not be represented in prognostic models of the Greenland Ice Sheet to
24 2100 and beyond.

25 **1 Introduction**

26 The Greenland Ice Sheet (GrIS) is a major source of global sea level rise (SLR) and contributed 171
27 Gt a⁻¹ ($\sim 0.47 \pm 0.23$ mm a⁻¹) to SLR between 1991 and 2015 (van den Broeke et al., 2016). Mass
28 loss has accelerated since the mid-1990s and coincided with both elevated atmospheric temperatures
29 (e.g. Hanna et al., 2012) and warmer oceanic waters reaching marine-terminating glacier margins
30 (e.g. Straneo and Heimbach, 2013). Approximately 40% of Greenland's mass loss since 1991 was
31 due to increased ice discharge from marine-terminating outlet glaciers and it accounted for ~60% of
32 ice loss during the phase of rapid outlet glacier retreat observed between 2000 and 2005 (Rignot and
33 Kanagaratnam, 2006; Enderlin et al., 2014; Anderson et al., 2015; van den Broeke et al., 2016). As
34 such, predictions of ice discharge from Greenland's marine-terminating outlet glaciers are critical for
35 forecasting near-future sea level rise. Despite their importance, substantial uncertainty remains over
36 the response of Greenland's outlet glacier to climatic and oceanic warming (e.g. Carr et al., 2013;
37 Enderlin et al., 2013; Stocker et al., 2013). This response is complicated by glacier-specific factors,

38 particularly the bed and fjord geometry, which can strongly enhance/suppress glacier response to
39 forcing (e.g. Moon et al., 2012; Carr et al., 2015).

40 Kangerdlugssuaq Glacier (68.5°N, 33.0°W; Kangerdlugssuaq herein), East Greenland, is one of
41 Greenland's largest tidewater glaciers, draining approximately 3 % of the total area of the ice sheet
42 (Bevan et al., 2012) and accounting for 5% of ice sheet discharge (Enderlin et al., 2014). Following a
43 period of sustained low-elevation thinning during the mid to late 1990s (Thomas et al., 2000; Khan et
44 al., 2014), Kangerdlugssuaq retreated abruptly by 5 km between April 2004 and April 2005
45 (Luckman et al., 2006; Howat et al., 2007). Coincident with this retreat, the glacier accelerated from
46 $\sim 7,500 \text{ m a}^{-1}$ ($\sim 20 \text{ m d}^{-1}$) to $\sim 13,000 \text{ m a}^{-1}$ ($\sim 35 \text{ m d}^{-1}$) (Luckman et al., 2006). Following the 2005
47 retreat, Kangerdlugssuaq decelerated and re-advanced by $\sim 2 \text{ km}$ between 2006 and 2010 (Howat et
48 al., 2007; Bevan et al., 2012). Ice losses returned to pre-retreat values by the summer of 2008 (Howat
49 et al., 2011). However, these changes in speed, frontal position, and subsequent diffusive thinning
50 (Stearns and Hamilton, 2007) resulted in mass loss of 80 Gt of ice between September 2004 and
51 January 2008; a three-fold increase on pre-retreat rates of ice loss (Howat et al., 2011). Between 2000
52 and 2012, Kangerdlugssuaq accounted for $\sim 14 \%$ ($\sim 105 \text{ Gt}$) of the total cumulative discharge
53 anomaly of the entire GrIS ($\sim 750 \text{ Gt}$; Enderlin et al., 2014) and was second only to Jakobshavn Isbrae
54 ($\sim 21 \%$; 158 Gt).

55 The most recent published records of Kangerdlugssuaq's variations in frontal-position and speed end
56 by 2012 (Bevan et al., 2012; Khan et al., 2014; Murray et al., 2015). Since then, Kangerdlugssuaq has
57 entered a new phase of rapid retreat. Here we present an intra-annual time-series of ice frontal
58 position between March 2013 and September 2018 from Landsat 8 satellite imagery. We couple this
59 time-series of ice frontal positions with ice velocity and surface elevation datasets to evaluate the
60 dynamic response of Kangerdlugssuaq to recent changes in terminus position. Finally, we discuss
61 local topographic setting as a control on recent and future glacier behaviour.

62 **2 Methods**

63 **2.1 Glacier frontal position**

64 Terminus positions of Kangerdlugssuaq were manually digitised from all available Level 1T
65 pansharpened (15 m) Landsat 8 Operational Land Imager (OLI) satellite imagery between 2013 and
66 2018 using the Google Earth Digitisation Tool (GEEDiT) (Lea, 2018). We visualised (within a web-
67 browser) every Landsat 8 image available between 20 March 2013 (first available Landsat 8 image
68 for Kangerdlugssuaq) and 03 September 2018 (end of study period), and manually digitised the
69 glacier termini for each image where an ice front was visible. The presence of year round mélange
70 precluded the mapping of part or all of the glacier terminus for some images. In such scenarios, only
71 the contiguous portion of the terminus that could be differentiated from the mélange was mapped.
72 Due to overlap in satellite tracks, where multiple images were available for the same day we
73 measured the ice front using the first image acquired unless there was any discernible change.
74 Mapped glacier termini were subsequently exported from GEEDiT in vector format as GeoJSON
75 files and were converted to ESRI Shapefiles using the Margin change Quantification Tool (MaQiT)
76 (Lea, 2018). As each terminus trace has metadata automatically appended within GEEDiT, including
77 the unique path identifier, it is possible to directly and easily identify the original image used in the
78 mapping; for example using GEEDiT Reviewer (Lea, 2018).

79 Changes in frontal position were assessed using the curvilinear box method in MaQiT (Lea, 2018).
80 This method is an extension of the commonly used 'box method' (e.g. Moon and Joughin, 2008), and
81 used a reference box of fixed width (3 km here) and upstream extent spanning the centre line that

82 intersects with contiguously mapped glacier termini. Any termini that did not fully cover the width of
83 the reference box were excluded from the analysis. Here we defined the centre line as the line
84 representing the midpoint between the 0 m elevation contour from the BedMachinev3 dataset (see
85 Section 2.4; Morlighem et al., 2017). The centre line was extracted by tracing the line following the
86 maximum Euclidean distance between the 0 m contour, from its furthest point up-glacier to an
87 arbitrary point beyond the glacier's maximum extent (Figure 1; e.g. Lea et al., 2014). Mean retreat
88 was subsequently calculated by normalising the change in reference box area by its width. This
89 method therefore captured spatially asymmetric retreat and advance of a calving margin (Moon and
90 Joughin, 2008). Based on the above method, from a possible 199 images, we obtained 124 terminus
91 traces between 2013 and 2018 (Figure S1 in the Supporting Material). Cloud and/or mélange
92 obscured imagery precluded a constant temporal sampling frequency. However, an average of ~20
93 ($\sim\sigma$ 8) terminus traces were obtained per year, with an average sampling frequency of ~15 days (σ
94 ~32). We coupled these newly-derived terminus positions with the datasets of Khan et al. (2014)
95 (annual 1932, 1966, 1972, 1981, 1985, 1991 and 1999 - 2012) and Murray et al. (2015) (seasonal
96 2000 - 2010) to provide historical (back to 1932) context to the ice front evolution of
97 Kangerdlugssuaq (Figure 1).

98 Uncertainty in ice front positions is attributed to error in both geolocational accuracy of imagery and
99 precision in manual digitisation of the ice fronts (e.g. Carr et al., 2015). The former was assessed by
100 digitising a section of rock coastline adjacent to the terminus of Kangerdlugssuaq for a sub-sample of
101 30 Landsat 8 images that covered the whole time-period and path/row combinations, using the
102 curvilinear box method, where there should be no discernible change between images (e.g. Bevan et
103 al., 2012; Carr et al., 2013). The mean error was ± 3.6 m. The latter was assessed by repeatedly
104 digitising the termini of the glacier 30 times in a single Landsat 8 image (e.g. Moon et al., 2015),
105 using the curvilinear box method, again there should be no discernible change. The mean error was \pm
106 2.5 m. Propagating these errors gives an overall mapping uncertainty of ± 4.4 m, which is less than
107 the pixel resolution (15 m) of our imagery.

108 2.2 Ice velocity

109 Datasets on ice velocity, basal topography and surface elevation change were compiled from publicly
110 available sources. Ice surface velocities for Kangerdlugssuaq were acquired from the MEaSUREs
111 (<https://nsidc.org/data/NSIDC-0481>) programme (Joughin et al., 2010; 2011). These velocity maps
112 were produced from 11 to 33 day Interferometric Synthetic Aperture Radar (InSAR) image pairs
113 measured by TerraSAR-X / TanDEM-X, and have a resolution of 100 m (Joughin et al., 2011). 172
114 velocity maps were available between February 2009 and November 2017 (Figures S2 and S3), with
115 an average of ~19 (σ ~7) velocity maps available per year. Velocity time-series were extracted from
116 fixed points along the ice flow centre line (Figure 1) at 100 m intervals (Figure 2). Velocity errors
117 were calculated using the dataset error values for each velocity maps (Joughin et al., 2011), and
118 resulted in a mean error of ± 11.5 m a⁻¹ for our centre line.

119 2.3 Surface elevation change

120 The rate of surface elevation change was determined using Operation IceBridge ATM L4 Surface
121 Elevation Rate of Change data (Studinger, 2014; <https://nsidc.org/data/IDHDT4>). Measurements
122 were made at all points where coincident Airborne Topographic Mapper (ATM) widescan ILATM1B
123 elevation data existed from two different campaigns, and were provided as average rate of change
124 (dH/dT) of the surface elevation between the two measurement times. Data availability varied
125 spatially and temporally, so values that exactly followed our centreline could not be extracted. To
126 overcome this, we assessed surface elevation change along the profiles where data were available for

127 each time step (Figure 3 and S4). We determined annual change for all available years ($n = 11$)
128 between 2017 and 2001, and cumulative change to a 2001 baseline ($n = 14$). The latter were
129 converted from average rate of change to cumulative elevation change using the time difference
130 information provided in the dataset's metadata. Using the dataset errors (Studinger, 2014) for all
131 points in our selected time periods, resulted in a mean error of ± 1.43 m for the annual change
132 datasets and ± 1.89 m for the cumulative change datasets.

133 2.4 Basal topography

134 Basal topography was acquired from the Operation IceBridge BedMachine v3 dataset
135 (<https://nsidc.org/data/IDBMG4>), which is derived from ice thickness and mass conservation, and is
136 coupled with ocean bathymetry to provide a 150 m resolution bed map of Greenland (Morlighem et
137 al., 2017). Bed topography was sampled at 150 m intervals along the centre line (Figure 4). Errors
138 were calculated using the dataset error values (Morlighem et al., 2017), and resulted in a mean error
139 of ± 84 m.

140 3 Results

141 Between 2013 and 2016 Kangerdlugssuaq's frontal position followed a typical seasonal progression:
142 before our first available position in late February the ice front advanced with limited calving
143 reaching a maximum position towards the middle of the year (~July; Figures 2c and S5). After this,
144 the ice front retreated, often via a series of large calving episodes, and retreat continued until at least
145 our last available frontal position in October/November (Figures 2c and S5). During each winter
146 (December to February), the ice front would re-advance so that the early spring terminus position
147 was seaward of the previous autumn position. This 2-3 km seasonal oscillation has been typical of
148 Kangerdlugssuaq since at least 1985 (Figure 2c; e.g. Luckman et al., 2006; Bevan et al., 2012;
149 Murray et al., 2015). However, the behaviour of the glacier changed markedly in winter 2016/2017,
150 when the ice front retreated by 2.5 km, rather than the usual winter advance (Figures 2c and S4). As a
151 result, the spring 2017 ice front was ~2.5 km behind the spring 2016 position (Figures 2c and S5). In
152 2017, the early season advance was interrupted by a series of calving events, limiting the seasonal
153 advance (Figures 2c and S5). During winter 2017, Kangerdlugssuaq's ice front underwent a second
154 phase of extended retreat through to May 2018, with total retreat of 3 km (Figures 2c and S5). This
155 brought the spring 2018 ice front ~2.5 km behind its position in spring 2017, and ~5 km behind its
156 location in spring 2016 (Figures 2c and S5). As in 2017, early seasonal advance in 2018 was
157 punctuated by further calving events. Kangerdlugssuaq has therefore entered a new phase of retreat,
158 which occurred through extended winter retreat and limited spring readvance in 2017 and 2018. This
159 retreat has brought Kangerdlugssuaq's ice front to its most retreated position since at least 1932
160 (Figure 1).

161 Our data demonstrate that Kangerdlugssuaq decelerated between 2011 and 2017, with peak summer
162 velocity reducing by $\sim 1,500$ m a^{-1} from $\sim 10,000$ m a^{-1} in 2011 to $\sim 8,500$ m a^{-1} in 2017. The glacier
163 then accelerated throughout 2017, such that early spring velocities ($\sim 8,500$ m a^{-1}) equalled the
164 previous year's summer velocities, reaching a peak velocity of $\sim 10,000$ m a^{-1} in November (Figure
165 2). This near-terminus (V0.5) November velocity was $\sim 2,500$ m a^{-1} above the previous year's
166 November velocity of $\sim 7,500$ m a^{-1} (Figure 2), representing a 33% increase. This velocity increase is
167 far greater than annual velocity cycles of the preceding years ($\sim 1,000$ m; Figure 2). Changes in
168 velocity were apparent at least 20 km inland of the terminus but were of highest amplitude nearer to
169 the ice front (Figure 2). Coincident with velocity change, near-terminus thinning of up to 10 m a^{-1}

170 occurred between 2017 and 2016, following three years of thickening for the periods of 2016-2015,
171 2015-2014 and 2014-2013 (Figure 3 and S4).

172 Given the influence of basal topography on the rate and extent of glacier retreat (e.g. Weertman,
173 1974; Thomas, 1979; Schoof, 2007) we investigated the position of the ice front with respect to basal
174 topography over time (Figure 4). Kangerlussauq currently terminates within an overdeepening.
175 Between 2013 and 2016 the ice front occupied a zone of flat-lying bed topography within this
176 overdeepening, ~850 m below sea level. Retreat during the winter of 2016 removed the ice front
177 from this flat-lying bed into the deepest parts of the overdeepening and onto a reverse bed slope.
178 Apart from one bedrock ridge across the fjord (~50 m in height; located at ~45 km in Figure 4) this
179 reverse slope continues to over 1,100 m below sea level, with the overdeepening extending ~15 km
180 inland before the bed slopes upward again (Figure 4). Retreat during 2017 also brought the glacier
181 front into the widest section of its fjord (~8.5 km wide; Figure 1).

182 **4 Discussion**

183 Our observations demonstrate that between 2016 and 2017 Kangerdlugssuaq's dynamics changed
184 substantially (Figures 2 and 3). Following a period of terminus advance between summer 2011 and
185 summer 2016, Kangerdlugssuaq's ice front rapidly retreated by 5 km between 2017 and 2018 (Figure
186 2). Although comparable rates of retreat have occurred at least twice since 1932 (Luckman et al.,
187 2006; Khan et al., 2014), this current phase retreated the terminus to the most inland position since
188 the earliest known observations in 1932 (Figure 1; Bevan et al., 2012; Khan et al., 2014). Following
189 late 2016/early 2017 retreat, Kangerdlugssuaq accelerated throughout 2017 (Figure 2) and began to
190 thin close to the terminus (Figure 3). This dynamic response has been observed on other Greenland
191 outlet glaciers, and stems from a loss of resistive stress at the glacier front, leading to ice
192 acceleration, thinning and further retreat (e.g. Howat et al., 2007; Stearns and Hamilton, 2007;
193 Joughin et al., 2010; Moon et al., 2012). As such, it can lead to feedbacks developing and major ice
194 loss (Thomas et al., 2011; Joughin et al., 2012).

195 Kangerdlugssuaq experienced similar retreat and acceleration to those observed in 2016/17 between
196 2004 and 2005 (e.g. Luckman et al., 2006). During 2004/2005, increases in speed, retreating frontal
197 position and subsequent diffusive thinning caused Kangerdlugssuaq to lose 80 Gt of ice before
198 returning to the pre-event balance rate (~6.5 Gt a⁻¹) in the summer of 2008. This enhanced period of
199 mass loss represented a three-fold increase in ice discharge when compared to pre-retreat rates of ice
200 loss (Howat et al., 2011). Other short-lived episodes of retreat have led to Kangerdlugssuaq monthly
201 loss rates exceeding 100 Gt a⁻¹ (Howat et al., 2011). Variations in ice discharge from
202 Kangerdlugssuaq therefore have substantial implications for total GrIS mass loss (e.g. Stearns and
203 Hamilton, 2007). The observed dynamical changes at Kangerdlugssuaq since 2016 are likely to lead
204 to an increase in discharge and contribution to global SLR over the next 1-5 years. Unlike the
205 2004/2005 event, where the glacier acceleration and retreat was short lived, and the glacier started to
206 decelerate and advance the following year (Howat et al., 2007; Bevan et al., 2012), recent retreat at
207 Kangerdlugssuaq has occurred over multiple years. If the associated acceleration in speed is
208 maintained, or increases, beyond 2018 then enhanced ice discharge and mass loss from
209 Kangerdlugssuaq could be sustainable for 5-20 years. At present, Jakobshavn Isbræ is the only
210 glacier on the GrIS that has experienced comparable sustained acceleration over multiple years (e.g.
211 Van der Veen et al., 2011; Joughin et al., 2012).

212 Fjord geometry (bed and width) is a very important control on recent fluctuations of
213 Kangerdlugssuaq's ice front and will continue to influence the glacier's near future behaviour. The

214 last major retreat event in 2005 left the terminus on the edge of a ~15 km long bedrock high (yellow
215 bar in Figure 4b). In contrast, the recent phase of retreat (from 2017) moved the terminus from this
216 bedrock high into an ~3 km long region of reverse bed slope that falls by ~150 m of elevation, and
217 into a wider section of the fjord (Figure 1 and red bar in Figure 4). Retreat down a reverse bedrock
218 slope can cause large increases in ice discharge, due to feedbacks between grounding line thickness,
219 terminus retreat, acceleration and dynamic thinning (Meier and Post, 1987; Schoof, 2007;
220 Gudmundsson et al., 2012). Theoretically, these feedbacks will only stop once the terminus reaches
221 an area of horizontal or forward-sloping bed (Weertman, 1974; Schoof, 2007; Gudmundsson et al.,
222 2012). Similarly, a terminus moving into a widening fjord can also promote enhanced ice discharge,
223 as the ice must thin to conserve mass and because lateral resistive stresses is inversely proportional to
224 width, meaning that the fjord walls will offer less resistance to flow in wider sections of the fjord
225 (Raymond, 1996; Jamieson et al., 2012; Carr et al., 2013). At present, the ice front appears to be
226 resting on a ~750 m wide, ~50 m high bedrock ridge, which may inhibit immediate rapid retreat into
227 the overdeepened trough (Figure 3) (e.g. Jamieson et al., 2012). However, bed elevation immediately
228 beyond this bump decreases for ~10 km inland from ~950 m to ~1,150 m below sea level. Although
229 upstream narrowing in fjord width could also modulate the rate of flow (e.g. Jamieson et al., 2012),
230 Kangerdlugssuaq's ice front is likely primed for further retreat to the head of this trough (Khan et al.,
231 2014). Unlike the 2005 retreat event where the glacier rapidly (1-2 years) re-adjusted to near-balance
232 following a perturbation in geometry (Howat et al., 2007), our observation of multi-year retreat,
233 coupled with a topographic profile that deepens significantly inland suggests that Kangerdlugssuaq is
234 likely to experience prolonged rapid retreat and accelerated ice flow, and thus enter an extended
235 phase of enhanced mass loss. Near-future change (retreat) in ice front position may therefore largely
236 be governed by changes in ice dynamics, with only a weak dependence on atmospheric or
237 oceanographic forcings.

238 Recent changes in Kangerdlugssuaq's dynamics are likely to have a number of implications for
239 regional and ice sheet-wide mass loss. At the basin scale, Kangerdlugssuaq dominates mass loss from
240 the eastern sector of the GrIS (basin 3 of Andersen et al., 2015). Unlike the majority of the GrIS, it is
241 ice dynamics and not surface mass balance that contributes the largest fractional proportion to mass
242 loss in this sector (Andersen et al., 2015). We expect this trend to continue in the near future. At the
243 ice sheet-scale, 80 % of total ice discharge is from glaciers in the south-east and north-west of
244 Greenland (Enderlin et al., 2014). These regions also accounted for 86 % of ice sheet wide increases
245 in ice discharge as it increased from 462 ± 6 Gt in 2000 to 546 ± 7 Gt in 2012 (Enderlin, et al., 2014).
246 Since 2006 discharge has stabilised in south-east Greenland following the slowdown of
247 Kangerdlugssuaq and Helheim Glaciers (e.g. Howat et al., 2007), and recent (2008-2012) increases in
248 GrIS discharge have been attributed to glaciers from the north-west (Enderlin et al., 2014). Given
249 Kangerdlugssuaq's impacts on both the magnitude and pattern of ice sheet wide mass loss (Rignot
250 and Kanagaratnam, 2006; Stearns and Hamilton, 2007; Enderlin et al., 2014), its new phase of
251 retreat, acceleration and thinning (Figures 2-4) is likely to markedly increase discharge from south-
252 east Greenland, and may result in the south-east region dominating future increases in discharge from
253 the GrIS.

254 **5 Conclusions**

255 We have shown that within the last two years, Kangerdlugssuaq has entered a new phase of rapid
256 retreat and acceleration, the second time this has occurred within the last two decades, and its ice
257 front is now at its most retreated position since at least the early 20th-century. This retreat has
258 brought Kangerdlugssuaq's ice front into a major (~15 km long) overdeepening. Coincident with
259 retreat, Kangerdlugssuaq accelerated and thinned near the terminus, and is likely to result in

260 substantial dynamic draw down and loss of ice to the oceans. Glacier geometry strongly modulates
261 Kangerdlugssuaq's behaviour. The phase of rapid 5 km retreat between 2016 and 2018 coincided
262 with the ice front moving from the edge of a bedrock high, to a region of reverse bed slope. Given the
263 proximity of the ice front to further reverse bed slope, further retreat would very likely result in ~10
264 km retreat to the head of this trough. Due to these uncertainties, high temporal resolution monitoring
265 of geometric, frontal position and velocity change, coupled with accurate bed topography, will be
266 critical for accurately predicting and quantifying future patterns of ice loss at Kangerdlugssuaq.
267 Given Kangerdlugssuaq's previous impacts on both the magnitude and pattern of ice sheet wide mass
268 loss, we predict that its new phase of retreat, acceleration and thinning will result in a switch back to
269 the south-east being the largest contributing region to increasing discharge from the GrIS. More
270 broadly, accurate forecasting of the GrIS's contribution to SLR will require a deeper understanding
271 of, and responses to, these non-linear ice dynamic processes.

272 **6 Conflict of Interest**

273 The authors declare that the research was conducted in the absence of any commercial or financial
274 relationships that could be construed as a potential conflict of interest.

275 **7 Author Contributions**

276 SB, RC, NR designed the study. JL wrote and provided the code for GEEDiT and MaQiT. SB
277 conducted all data analysis and led the writing of the manuscript. RC, NR and JL gave conceptual
278 and technical advice, and edited the manuscript.

279 **8 Funding**

280 SB, RC and NR gratefully acknowledge support from Newcastle University through its Research
281 Excellence Academy funding scheme, which supported SB's postdoctoral position.

282 **9 Acknowledgments**

283 We acknowledge a number of freely available datasets used in this study. We are grateful to Khan et
284 al. (2014) and Murray et al. (2015) for making available historical terminus data; Joughin et al.
285 (2010) for velocity and Howat et al. (2014) for surface topography data, both available as part of the
286 MEaSURES programme; and Morlighem et al. (2017) and Studinger (2014) for topographic and
287 surface elevation change data, both available as port of Operation IceBridge.

288 **10 Data Availability Statement**

289 A shapefile of frontal positions for Kangerdlugssuaq between 2013 and 2018 is included in the
290 supporting material to this article. All other data sources – including satellite imagery, InSAR
291 velocity maps, surface elevation, surface elevation change and bed topography – are freely available
292 online. The sources for these datasets are provided in text and subsequent reference list.

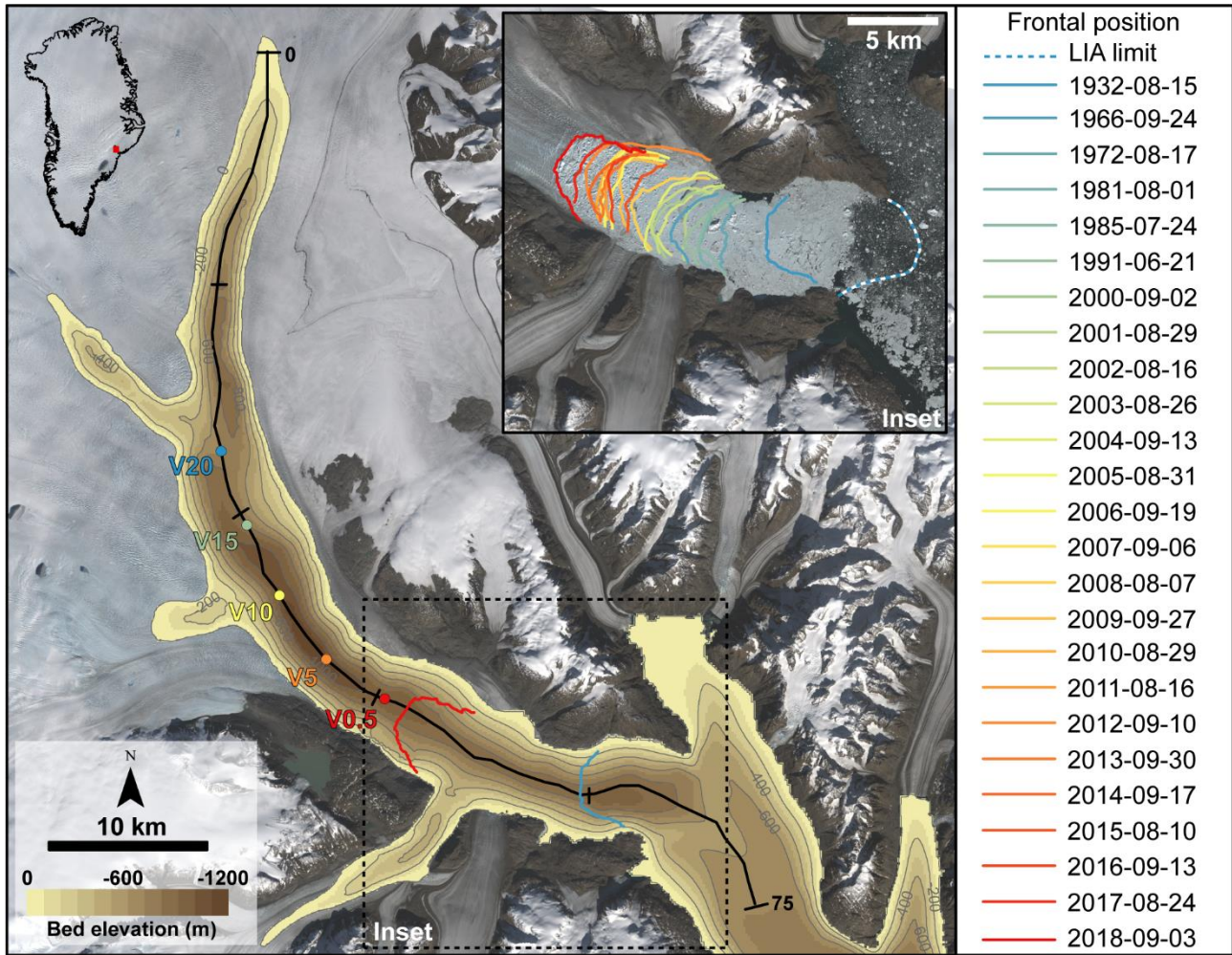
293 **11 References**

294 Andersen, M.L., Stenseng, L., Skourup, H., Colgan, W., Khan, S.A., Kristensen, S.S., et al. (2015).
295 Basin-scale partitioning of Greenland ice sheet mass balance components (2007–2011). *Earth and*
296 *Planetary Science Letters* 409, 89-95. doi: 10.1016/j.epsl.2014.10.015.

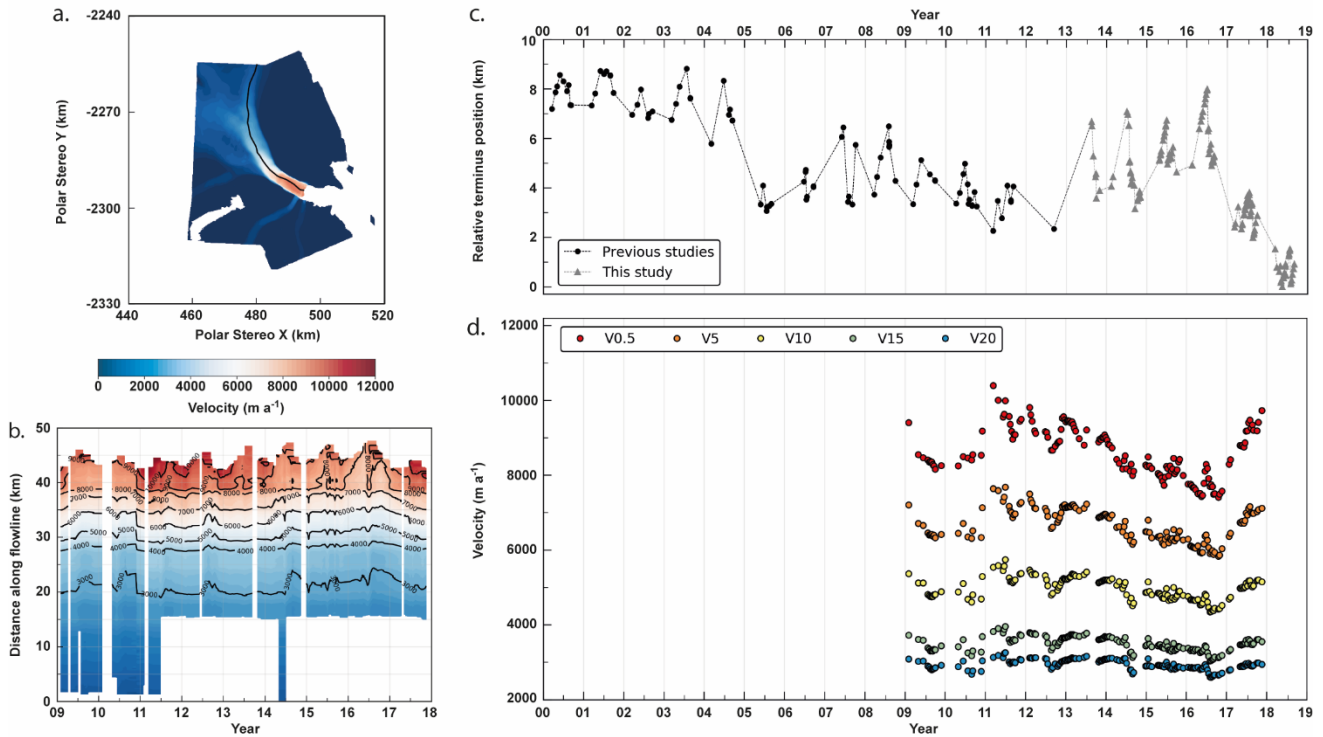
- 297 Bevan, S.L., Luckman, A.J., and Murray, T. (2012). Glacier dynamics over the last quarter of a
298 century at Helheim, Kangerdlugssuaq and 14 other major Greenland outlet glaciers. *The Cryosphere*
299 6(5), 923-937. doi: 10.5194/tc-6-923-2012.
- 300 Carr, J.R., Vieli, A., and Stokes, C. (2013). Influence of sea ice decline, atmospheric warming, and
301 glacier width on marine-terminating outlet glacier behavior in northwest Greenland at seasonal to
302 interannual timescales. *Journal of Geophysical Research: Earth Surface* 118(3), 1210-1226. doi:
303 doi:10.1002/jgrf.20088.
- 304 Carr, J.R., Vieli, A., Stokes, C.R., Jamieson, S.S.R., Palmer, S.J., Christoffersen, P., et al. (2015).
305 Basal topographic controls on rapid retreat of Humboldt Glacier, northern Greenland. *Journal of*
306 *Glaciology* 61(225), 137-150. doi: 10.3189/2015JoG14J128.
- 307 Enderlin, E.M., Howat, I.M., Jeong, S., Noh, M.-J., van Angelen, J.H., and van den Broeke, M.R.
308 (2014). An improved mass budget for the Greenland ice sheet. *Geophysical Research Letters* 41(3),
309 866-872. doi: 10.1002/2013GL059010.
- 310 Enderlin, E.M., Howat, I.M., and Vieli, A. (2013). High sensitivity of tidewater outlet glacier
311 dynamics to shape. *The Cryosphere* 7(3), 1007-1015. doi: 10.5194/tc-7-1007-2013.
- 312 Gudmundsson, G.H., Krug, J., Durand, G., Favier, L., and Gagliardini, O. (2012). The stability of
313 grounding lines on retrograde slopes. *The Cryosphere* 6(6), 1497-1505. doi: 10.5194/tc-6-1497-2012.
- 314 Hanna, E., H. Mernild, S., Cappelen, J., and Steffen, K. (2012). Recent warming in Greenland in a
315 long-term instrumental (1881–2012) climatic context: I. Evaluation of surface air temperature
316 records. *Environmental Research Letters* 7(4), 045404. doi: 10.1088/1748-9326/7/045404.
- 317 Howat, I.M., Ahn, Y., Joughin, I., van den Broeke, M.R., Lenaerts, J.T.M., and Smith, B. (2011).
318 Mass balance of Greenland's three largest outlet glaciers, 2000–2010. *Geophysical Research Letters*
319 38(12). doi: 10.1029/2011GL047565.
- 320 Howat, I.M., Joughin, I., and Scambos, T.A. (2007). Rapid Changes in Ice Discharge from Greenland
321 Outlet Glaciers. *Science* 315(5818), 1559-1561. doi: 10.1126/science.1138478/78.
- 322 Howat, I. M., Negrete, A., and Smith, B. E.: The Greenland Ice Mapping Project (GIMP) land
323 classification and surface elevation data sets, *The Cryosphere*, 8, 1509-1518, doi:10.5194/tc-8-1509-
324 2014, 2014.
- 325 Jamieson, S.S.R., Vieli, A., Livingstone, S.J., Cofaigh, C.Ó., Stokes, C., Hillenbrand, C.-D., et al.
326 (2012). Ice-stream stability on a reverse bed slope. *Nature Geoscience* 5, 799-802. doi:
327 10.1038/ngeo1600
- 328 Joughin, I., Smith, B.E., Howat, I.M., Floricioiu, D., Alley, R.B., Truffer, M., et al. (2012). Seasonal
329 to decadal scale variations in the surface velocity of Jakobshavn Isbrae, Greenland: Observation and
330 model-based analysis. *Journal of Geophysical Research: Earth Surface* 117(F2). doi:
331 10.1029/2011JF002110.
- 332 Joughin, I., Howat, I. M., Smith, B. E., and Scambos, T. (2011, updated 2018) MEaSUREs
333 Greenland Ice Velocity: Selected Glacier Site Velocity Maps from InSAR, Version 1.2. [subset:
334 Ecoast-68.80N]. Boulder, Colorado USA. NASA National Snow and Ice Data Center Distributed

- 335 Active Archive Center. doi: <https://doi.org/10.5067/MEASURES/CRYOSPHERE/nsidc-0481.001>.
336 [accessed: 17 August 2018].
- 337 Joughin, I., Smith, B.E., Howat, I.M., Scambos, T., and Moon, T. (2010). Greenland flow variability
338 from ice-sheet-wide velocity mapping. *Journal of Glaciology* 56(197), 415-430. doi:
339 10.3189/002214310792447734.
- 340 Khan, S.A., Kjeldsen, K.K., Kjær, K.H., Bevan, S., Luckman, A., Aschwanden, A., et al. (2014).
341 Glacier dynamics at Helheim and Kangerdlugssuaq glaciers, southeast Greenland, since the Little Ice
342 Age. *The Cryosphere* 8(4), 1497-1507. doi: 10.5194/tc-8-1497-2014.
- 343 Lea, J.M. (2018). The Google Earth Engine Digitisation Tool (GEEDiT) and the Margin change
344 Quantification Tool (MaQiT) – simple tools for the rapid mapping and quantification of changing
345 Earth surface margins. *Earth Surf. Dynam.* 6(3), 551-561. doi: 10.5194/esurf-6-551-2018.
- 346 Lea, J.M., Mair, D.W.F., and Rea, B.R. (2014). Evaluation of existing and new methods of tracking
347 glacier terminus change. *Journal of Glaciology* 60(220), 323-332. doi: 10.3189/2014JoG13J061.
- 348 Luckman, A., Murray, T., de Lange, R., and Hanna, E. (2006). Rapid and synchronous ice-dynamic
349 changes in East Greenland. *Geophysical Research Letters* 33(3). doi: doi:10.1029/2005GL025428.
- 350 Meier, M.F., and Post, A. (1987). Fast tidewater glaciers. *Journal of Geophysical Research: Solid*
351 *Earth* 92(B9), 9051-9058. doi: doi:10.1029/JB092iB09p09051.
- 352 Moon, T., and Joughin, I. (2008). Changes in ice front position on Greenland's outlet glaciers from
353 1992 to 2007. *Journal of Geophysical Research: Earth Surface* 113(F2). doi: 10.1029/2007JF000927.
- 354 Moon, T., Joughin, I., and Smith, B. (2015). Seasonal to multiyear variability of glacier surface
355 velocity, terminus position, and sea ice/ice mélange in northwest Greenland. *Journal of Geophysical*
356 *Research: Earth Surface* 120(5), 818-833. doi: 10.1002/2015JF003494.
- 357 Moon, T., Joughin, I., Smith, B., and Howat, I. (2012). 21st-Century Evolution of Greenland Outlet
358 Glacier Velocities. *Science* 336(6081), 576-578. doi: 10.1126/science.1219985.
- 359 Morlighem, M., Williams, C.N., Rignot, E., An, L., Arndt, J.E., Bamber, J.L., et al. (2017).
360 BedMachine v3: Complete Bed Topography and Ocean Bathymetry Mapping of Greenland From
361 Multibeam Echo Sounding Combined With Mass Conservation. *Geophysical Research Letters*
362 44(21), 11,051-011,061. doi: 10.1002/2017GL074954.
- 363 Murray, T., Scharrer, K., Selmes, N., Booth, A.D., James, T.D., Bevan, S.L., et al. (2015). Extensive
364 retreat of Greenland tidewater glaciers, 2000–2010. *Arctic, Antarctic, and Alpine Research* 47(3),
365 427-447. doi: 10.1657/AAAR0014-049.
- 366 Raymond, C. (2017). Shear margins in glaciers and ice sheets. *Journal of Glaciology* 42(140), 90-
367 102. doi: 10.3189/S0022143000030550.
- 368 Rignot, E., and Kanagaratnam, P. (2006). Changes in the Velocity Structure of the Greenland Ice
369 Sheet. *Science* 311(5763), 986-990. doi: 10.1126/science.1121381.

- 370 Schoof, C. (2007). Ice sheet grounding line dynamics: Steady states, stability, and hysteresis. *Journal*
371 *of Geophysical Research: Earth Surface* 112(F3). doi: 10.1029/2006JF000664.
- 372 Stearns, L.A., and Hamilton, G.S. (2007). Rapid volume loss from two East Greenland outlet glaciers
373 quantified using repeat stereo satellite imagery. *Geophysical Research Letters* 34(5). doi:
374 doi:10.1029/2006GL028982.
- 375 Stocker, T. F., Qin, D., Plattner, G.-K., Tignor, M. M. B., Allen, S. K., Boschung, J., Nauels, A., Xia,
376 Y., Bex, V., and Midgley, P. M. (eds.) (2013) *Climate change 2013: The Physical Science Basis.*
377 *Contribution of Working Group I to the Fifth Assessment Report of the Intergovernmental Panel on*
378 *Climate Change.* Cambridge University Press, Cambridge and New York, 1535pp.,
- 379 Straneo, F., and Heimbach, P. (2013). North Atlantic warming and the retreat of Greenland's outlet
380 glaciers. *Nature* 504, 36-43. doi: 10.1038/nature12854.
- 381 Studinger, M..(2014, updated 2018) IceBridge ATM L4 Surface Elevation Rate of Change, Version
382 1. [Subsets: 2013.04.02, 2014.03.12, 2015.04.08, 2016.05.09]. Boulder, Colorado USA. NASA
383 National Snow and Ice Data Center Distributed Active Archive Center. doi:
384 <https://doi.org/10.5067/BCW6CI3TXOCY>. [Accessed: 02 September 2018].
- 385 Thomas, R., Frederick, E., Li, J., Krabill, W., Manizade, S., Paden, J., et al. (2011). Accelerating ice
386 loss from the fastest Greenland and Antarctic glaciers. *Geophysical Research Letters* 38(10). doi:
387 10.1029/2011GL047304.
- 388 Thomas, R.H. (1979). The Dynamics of Marine Ice Sheets. *Journal of Glaciology* 24(90), 167-177.
389 doi: 10.3189/S0022143000014726.
- 390 Thomas, R.H., Abdalati, W., Akins, T.L., Csatho, B.M., Frederick, E.B., Gogineni, S.P., et al.
391 (2000). Substantial thinning of a major east Greenland outlet glacier. *Geophysical Research Letters*
392 27(9), 1291-1294. doi: 10.1029/1999GL008473.
- 393 van den Broeke, M.R., Enderlin, E.M., Howat, I.M., Kuipers Munneke, P., Noël, B.P.Y., van de
394 Berg, W.J., et al. (2016). On the recent contribution of the Greenland ice sheet to sea level change.
395 *The Cryosphere* 10(5), 1933-1946. doi: 10.5194/tc-10-1933-2016.
- 396 Van Der Veen, C.J., Plummer, J.C., and Stearns, L.A. (2017). Controls on the recent speed-up of
397 Jakobshavn Isbræ, West Greenland. *Journal of Glaciology* 57(204), 770-782. doi:
398 10.3189/002214311797409776.
- 399 Weertman, J. (1974). Stability of the Junction of an Ice Sheet and an Ice Shelf. *Journal of Glaciology*
400 13(67), 3-11. doi: 10.3189/S0022143000023327.

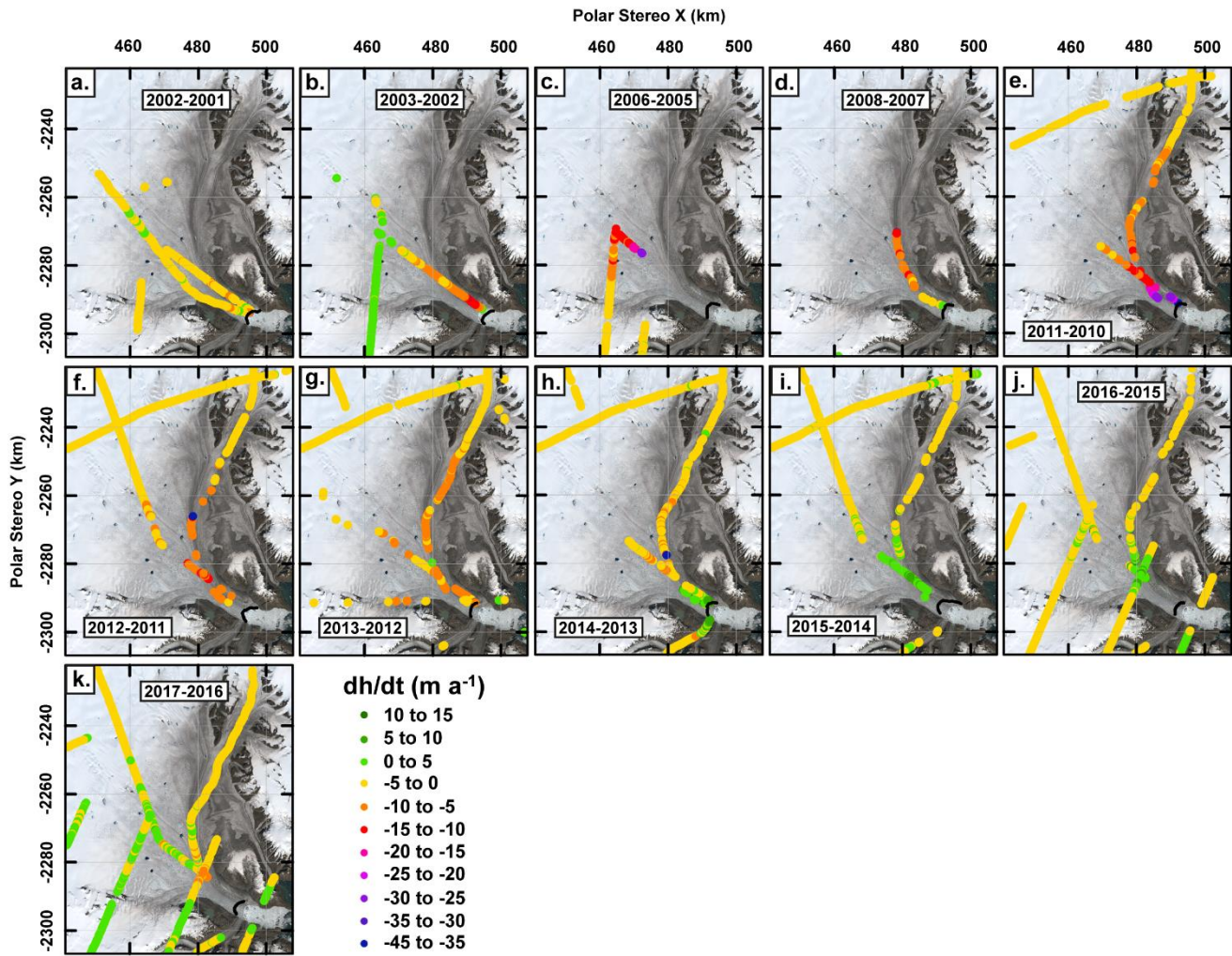


401
 402 **Figure 1:** Overview of Kangerdlugssuaq Glacier and mapped historical terminus positions (inset).
 403 Black line indicated the centre line profile plotted in Figures 2 and 3. Points V0.5 – V20 mark the
 404 locations for the velocity series shown in Figure 2d and indicate the distance (in km) from the most
 405 retreated ice front (16 May 2018). Annual ice fronts combine data from this study between 2013 and
 406 2018 and Khan et al. (2014) between 1932 and 2012. Background image is Landsat 8 scene from 03
 407 November 2018 (path 231 and row 012).



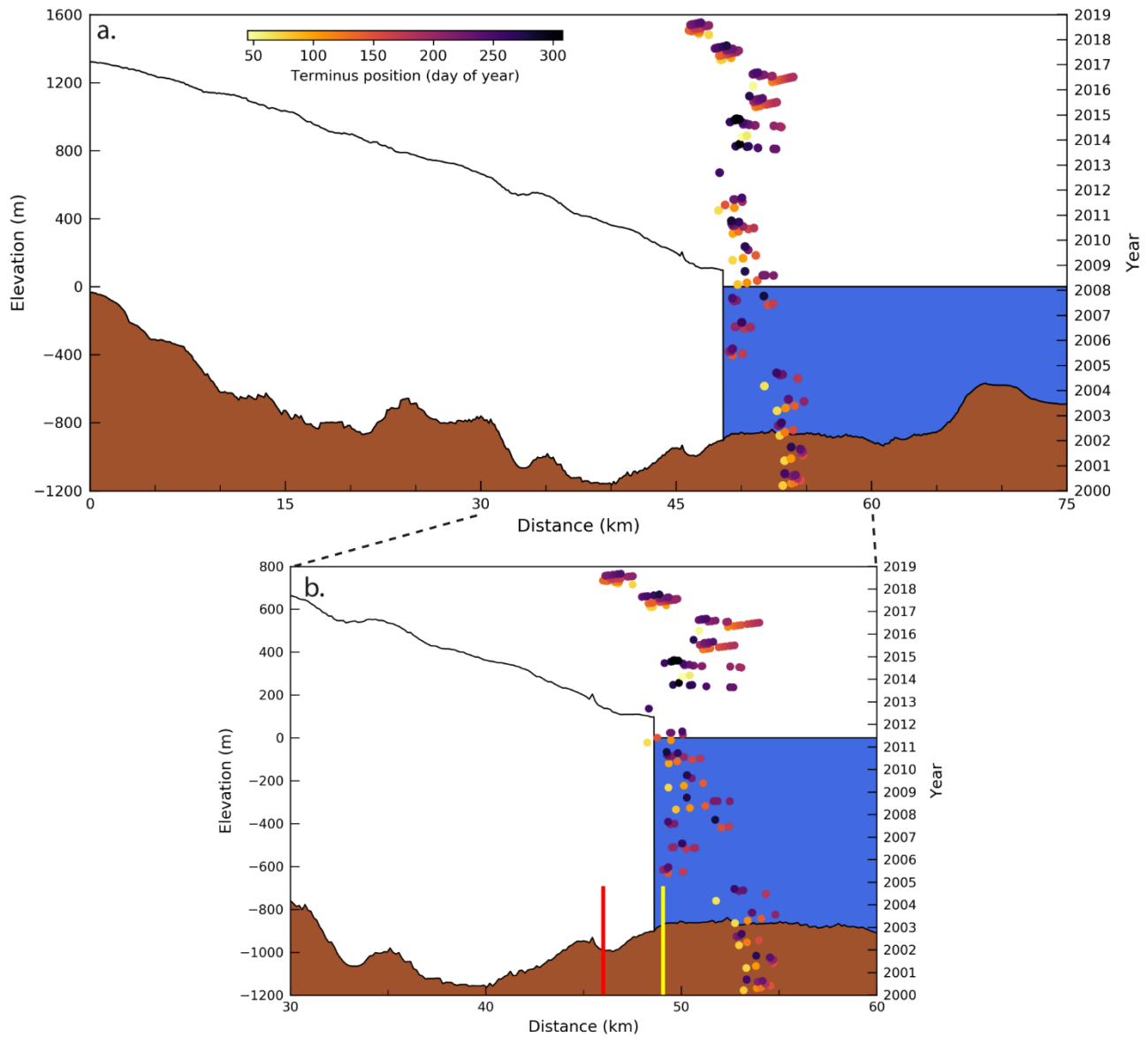
408
 409 **Figure 2:** Terminus and velocity change for Kangerdlugssuaq. (a) Mean glacier velocity between
 410 2009 and 2017. (b) Contour plot of along glacier velocity profile for centre line shown in (a). For
 411 visualisation purposes, and to obtain a more complete velocity record that accounts for unequal
 412 sampling periods between observations, the later were linearly interpolated if there were fewer than
 413 66 days between observations (i.e. six repeat pass cycles). (c) Change in terminus position between
 414 2000 and 2018. (d) Plots of velocity for selected points along the centre line as shown in Figure 1.
 415 Points were coded such that the numerical designation (e.g. V5) indicates the distance in kilometres
 416 from the most retreated ice front (16 May 2018).

Exceptional retreat of Kangerdlugssuaq Glacier



417
 418 **Figure 3:** Annual elevation change for Kangerdlugssuaq between 2001 and 2017. Panels relate to
 419 surface elevation change for the time periods 2002-2001 (a), 2003-2002 (b) 2006-2005 (c), 2008-
 420 2007 (d), 2011-2010 (e), 2012-2011 (f), 2013-2012 (g), 2014-2013 (h), 2015-2014 (i), 2016-2015 (j),
 421 2017-2016 (k). The most retreated terminus position for the given time period is demarcated in black.

Exceptional retreat of Kangerdlugssuaq Glacier



422
423 **Figure 4:** Bed and surface profiles of Kangerdlugssuaq along the centre line shown in Figure 1. (a)
424 Bed and surface profiles overlain with terminus positions between 2000 and 2018. Terminus
425 positions are coloured by day of year. (b) Near-terminus view of (a). The maximum retreat for the
426 years 2005 (yellow) and 2018 (red) are indicated by vertical lines. Surface elevation data is obtained
427 from the Greenland Ice Mapping Project (GIMP) surface digital elevation model, and has a nominal
428 date of 2007 (Howat et al., 2014).